metals

MDPI

Article

Joining Ti6Al4V to Alumina by Diffusion Bonding Using Titanium Interlayers

Marcionilo Silva, Jr. [1,2,3,4], Ana S. Ramos [4] and Sónia Simões [2,3,*]

[1] Department of Mechanical Engineering, Federal University of Amazonas, General Rodrigo Octavio Jordão Ramos ST, Manaus 69067-005, Brazil; marcionilo@ufam.edu.br
[2] DEMM, Department of Metallurgical and Materials Engineering, University of Porto, R. Dr. Roberto Frias, 4200-465 Porto, Portugal
[3] LAETA/INEGI, Institute of Science and Innovation in Mechanical and Industrial Engineering, R. Dr. Roberto Frias, 4200-465 Porto, Portugal
[4] University of Coimbra, CEMMPRE, Department of Mechanical Engineering, R. Luís Reis Santos, 3030-788 Coimbra, Portugal; sofia.ramos@dem.uc.pt
* Correspondence: ssimoes@fe.up.pt; Tel.: +351-225081424

Abstract: This work aims to investigate the joining of Ti6Al4V alloy to alumina by diffusion bonding using titanium interlayers: thin films (1 µm) and commercial titanium foils (5 µm). The Ti thin films were deposited by magnetron sputtering onto alumina. The joints were processed at 900, 950, and 1000 °C, dwell time of 10 and 60 min, under contact pressure. Experiments without interlayer were performed for comparison purposes. Microstructural characterization of the interfaces was conducted by optical microscopy (OM), scanning electron microscopy (SEM) with energy dispersive X-ray spectroscopy (EDS), and electron backscatter diffraction (EBSD). The mechanical characterization of the joints was performed by nanoindentation to obtain hardness and reduced Young's modulus distribution maps and shear strength tests. Joints processed without interlayer have only been achieved at 1000 °C. Conversely, joints processed using Ti thin films as interlayer showed promising results at temperatures of 950 °C for 60 min and 1000 °C for 10 and 60 min, under low pressure. The Ti adhesion to the alumina is a critical aspect of the diffusion bonding process and the joints produced with Ti freestanding foils were unsuccessful. The nanoindentation results revealed that the interfaces show hardness and reduced Young modulus, which reflect the observed microstructure. The average shear strength values are similar for all joints tested (52 ± 14 MPa for the joint processed without interlayer and 49 ± 25 MPa for the joint processed with interlayer), which confirms that the use of the Ti thin film improves the diffusion bonding of the Ti6Al4V alloy to alumina, enabling a decrease in the joining temperature and time.

Keywords: diffusion bonding; thin film; titanium; Al_2O_3; sputtering

Citation: Silva, M., Jr.; Ramos, A.S.; Simões, S. Joining Ti6Al4V to Alumina by Diffusion Bonding Using Titanium Interlayers. *Metals* **2021**, *11*, 1728. https://doi.org/10.3390/met11111728

Academic Editor: Daolun Chen

Received: 28 September 2021
Accepted: 25 October 2021
Published: 29 October 2021

1. Introduction

Ti6Al4V is the most used commercial titanium alloy due to its excellent performance and attractive properties, such as high-temperature specific strength, low density, excellent creep, and corrosion resistance [1]. Combining this titanium alloy with advanced ceramics, e.g., alumina (Al_2O_3), which has high thermal stability, excellent wear and corrosion resistance, and chemical inertness [2], can be interesting for applications in the medical, aircraft, nuclear and micro-electro-mechanical systems (MEMS) sectors [1,3–6]. However, obtaining sound joints with good mechanical properties between titanium alloys and ceramic materials has been challenging due to their different properties, e.g., thermal conductivity, coefficient of thermal expansion (CTE), and chemical properties. This mismatch of properties induces the formation of residual stresses at the joint's interface during cooling. Researchers have worked to improve knowledge about the mechanisms that affect the joining of metals to ceramics [7–14]. The most reported technologies in the literature with

regards to joining dissimilar materials are brazing and solid-state diffusion bonding [15–17]. Brazing [18–28] is an attractive process that consists of adding a filler metal between the base materials. Ag-based commercial alloys can be used successfully as brazing alloys since they improve the reaction between metal and ceramic and enhance wetting [29]. However, this brazing alloy produces an interface with a lower service temperature than the titanium alloy. Furthermore, heterogeneous interfaces at microstructure and chemical composition level are formed, and post-processing heat treatments are necessary [30]. Diffusion bonding can obtain sound joints between dissimilar materials, mainly when interlayers are applied to join the faying diffusion surfaces. In this case, cracks due to residual stress can be prevented [10,17,31–38]. Active elements have been used as interlayers, e.g., titanium, niobium, and zirconium [15,16]. Titanium is the most used interlayer; for instance, it reacts with Al_2O_3 by diffusion bonding resulting in the formation of TiO, TiAl, and Ti_3Al [8]. The use of interlayers in diffusion bonding can be one option to reduce the bonding temperature, pressure and time and make the process more industrially attractive [39]. This may be even more important in metal-ceramic joining, when the joint is subjected to thermal cycling or thermal shock, large stress concentrations may be introduced in parts of the ceramic.

Researchers have been working to improve the joining between dissimilar materials by diffusion bonding. Barrena et al. [40] investigated the joining of Ti6Al4V to Al_2O_3 by diffusion bonding using as interlayer an Ag-Cu alloy (72 wt.% Ag, 28 wt.% Cu) with a thickness of 60 μm produced by electron beam evaporation. The interface's microstructure was composed of different Ti-Cu phases and (Ag), and the shear tests showed a maximum of 140 MPa obtained at a temperature of 750 °C and a dwell time of 30 min. Yu et al. [10] joined Ti6Al4V to Ti_2SnC using Cu foil (50 μm) as an interlayer in Ar atmosphere performed at a temperature of 750 °C during 60 min; a relatively low temperature was allowed due to the destabilization of Ti_2SnC that occurs below 700 °C. The interface's microstructure is formed mainly by Ti_3Cu_4 and $TiCu_4$, and the maximum value obtained at the shear tests was around 86 MPa [10]. Kliauga and Ferrante [41] joined Al_2O_3 to AISI304 stainless steel using a commercial Ti sheet with a thickness of 500 μm by diffusion bonding processed at 800 °C during 180 min and at 900 and 1000 °C during 120 min under a pressure of 15 MPa in vacuum. The authors investigated the interfacial reaction products of Ti/Al_2O_3. The microstructure characterization of the surface fracture showed that the composition depends on the temperature and dwell time. The joints produced at a temperature of 800 °C for 180 min exhibit the Ti_3Al phase at the interface close to the titanium base material, while TiAl is observed on the ceramic side. However, for joints obtained at 900 and 1000 °C during 120 min, the interface is constituted only by Ti_3Al. In similar work, Travessa and Ferrante [42] diffusion bonded the same base materials and interlayer at 700 °C for 120 min, and 800 °C for 15 and 120 min. The experiments were unsuccessful, and no reaction could be seen at the interface. Rocha et al. [43] joined pure Ti to Al_2O_3 by diffusion bonding at 800 °C for 90 min under a pressure of 5 MPa. The characterization of the Ti/Al_2O_3 interface identified the presence of TiAl adjacent to alumina and Ti_3Al adjacent to pure Ti. In addition, the authors applied galvanic corrosion tests to study the chemical degradation of the interfaces, and the results showed that the corrosion resistance was impaired by the TiAl phase. During the joining of Ti to Al_2O_3, TiAl intermetallic phase always comes up in zones adjacent to alumina, and the $TiAl/Ti_3Al$ ratio can increase with the thickness of the Ti interlayer [44].

Although some works referred to low temperature bonding (750–800 °C), the development of new approaches should be investigated to reduce the formation of (Ag) at the interface, as is the case when Ag-based alloys are used as interlayers. The presence of (Ag) is detrimental to the service temperature and should be avoided.

The objective of the present work consists in the study of the feasibility of joining Ti6Al4V to Al_2O_3 by diffusion bonding using titanium as interlayer material. Different titanium interlayers were investigated: Ti thin films deposited onto Al_2O_3 base material by magnetron sputtering and freestanding Ti thin foils. The joints processed using Ti foils

have a lower processing cost and are more straightforward than those using thin films obtained by magnetron sputtering. However, the lack of adhesion between the Ti foils and ceramics might make it difficult to get sound joints. The Ti interlayer was selected to allow an interface with a chemical composition similar to one of the base materials, avoiding the formation of phases that will impair the service temperature and with characteristics that promote the diffusion, enabling a decrease in the diffusion bonding processing conditions. Joining without interlayer was also conducted using the same parameters to evaluate the potential of these interlayers. The microstructural characterization of the joints' interface was carried out by optical microscopy (OM), scanning electron microscopy (SEM), energy dispersive X-ray spectroscopy (EDS), and electron backscatter diffraction (EBSD), while the mechanical characterization was performed by nanoindentation tests across the joints' interface and shear strength tests.

2. Materials and Methods

2.1. Base Materials

Ti6Al4V alloy and polycrystalline Al_2O_3 (purity of 99%) were purchased from Goodfellow in rods with 7 and 6 mm diameters, respectively. They were cut 5 mm in length, ground, and polished down to 1 µm diamond suspension and 0.03 µm silica using standard metallographic procedure, then cleaned with deionized water, acetone, and ethanol in an ultrasonic bath and dried with heat blow air. The results of the polishing were assessed by optical microscopy (OM) (DM4000, Leica Microsystems, Wetzlar, Germany) and average roughness (Ra) of the surfaces was measured by profilometry (Perthometer SP4, with laser probe (Mahr Perthometer SP4, Göttingem, Germany)).

2.2. Titanium Interlayer

The titanium thin films were deposited onto the polished surfaces of alumina (substrate) by direct current magnetron sputtering using a Ti (99.99% pure) target (150 mm × 150 mm × 6 mm thick). After achieving a base pressure below 5×10^{-4} Pa in the sputtering chamber, Ar was introduced (P ~ 1.5×10^{-1} Pa). The substrate materials were cleaned by heating followed by Ar+ (current of 20 A) etching using an ion gun. To avoid residual impurities from the substrates, assuring a good adhesion between the substrate and the Ti film, the total etching time employed was increased to 12–10 min higher than the usual conditions. The deposition starts once the cleaning of the substrate is concluded, after introducing more argon into the sputtering chamber (4.0×10^{-1} Pa deposition pressure). The power density applied to the Ti target was 6.70×10^{-2} W·mm^{-2}. The Ti films were produced using a substrate rotation speed of ~23 rpm and a deposition time of 20 min to achieve a thickness of ~1.0 µm. The titanium foil was purchased from Goodfellow with a purity of 99.6%, dimensions of 25 mm × 25 mm, and thickness of 5 µm. For the joining experiments, the foil was cut into rectangular parts with sizes of 7 mm × 7 mm.

2.3. Adhesion

The adhesion strength between the Ti thin films and Al_2O_3 was measured by a pull-off test using an apparatus as referred to in [45,46]; however, the substrate has a surface area three times higher than in the literature. The test consists of gluing the film deposited onto the alumina substrate to a rigid rod, following the curing time of the glue. Then, the set was fixed by the grips of a tensile test machine. The tensile tests were carried out under environmental conditions using a load cell of 500 N and a loading speed of 10 µm/min. The adhesion strength was estimated for three specimens to obtain the average value.

2.4. Diffusion Bonding

Ti6Al4V and Al_2O_3 joining was performed in a tubular horizontal furnace (Termolab Electrical Furnace, Agueda, Portugal) under a vacuum level of 10^{-2} Pa. Figure 1 displays the device used to assure contact pressure of the faying surfaces. The dissimilar base

materials were joined with and without Ti interlayer, and diffusion bonding was carried out at 900, 950, and 1000 °C, during 10 and 60 min. The heating and cooling rates were 5 and 3 °C/ min, respectively.

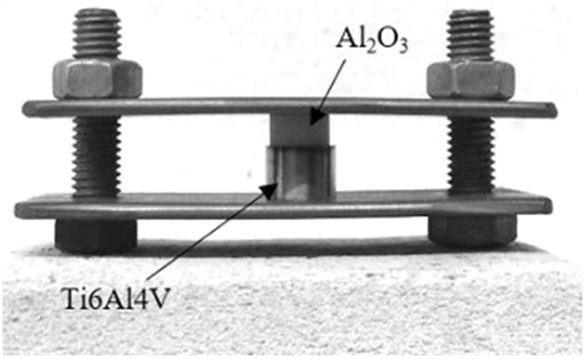

Figure 1. Device used to apply the contact pressure at the faying surfaces during the diffusion bonding experiments.

2.5. Microstructural Characterization

Optical microscopy (OM) was used to overview the soundness of the joints' interface. A DM 4000 M optical microscope equipped with a Leica DFC 420 camera (Leica Microsystems, Wetzlar, Germany) was used to achieve this objective.

For the microstructural and chemical characterization, cross-sections of the joints were prepared using standard metallographic techniques. Afterward, the joints' interfaces were analyzed by scanning electron microscopy (SEM) (FEI Quanta 400FEG ESEM/EDAX Genesis X4M (FEI Company, Hillsboro, OR, USA)) operating at an accelerating voltage of 15 keV, coupled with energy dispersive X-ray spectroscopy (EDS) (Oxford Instrument, Oxfordshire, UK) by the standardless quantification method. Electron backscatter diffraction (EBSD) analyses were conducted using an acceleration voltage of 15 keV to obtain Kikuchi patterns using a detector TSL-EDAX EBSD Unit (EDAX Inc. (Ametek), Mahwah, NJ, USA), allowing the phases in localized zones of the interfaces to be identified. The indexation of the patterns was made by ICDD PDF2 (2006) database.

2.6. Mechanical Characterization

Hardness and reduced Young's modulus were evaluated across the joints by nanoindentation. The experiments were carried out in a computer-controlled apparatus equipped with a Berkovich diamond indenter (NanoTest, Micro Materials Limited, Wrexham, UK). A maximum load of 5 mN was selected, and 8 × 12 matrices were defined, starting on the Ti6Al4V side, crossing the joints' interface, and moving towards the alumina base material. The distances between rows and columns were 5 and 3 µm, respectively. Loading/unloading was carried out in 30 s, with 30 s at maximum load and at 10% of maximum load during unloading for thermal drift correction. Hardness and reduced Young's modulus were determined by the Oliver and Pharr method [47].

Mechanical characterization was also performed by shear tests; three specimens were tested at room temperature at a rate of 1 mm/min for each joint. Figure 2 shows the shear strength apparatus used in this investigation and a schematic illustration. The fracture surface of the joints submitted to shear strength tests was evaluated by digital microscope DVM6 (Leica Microsystems, Wetzlar, Germany).

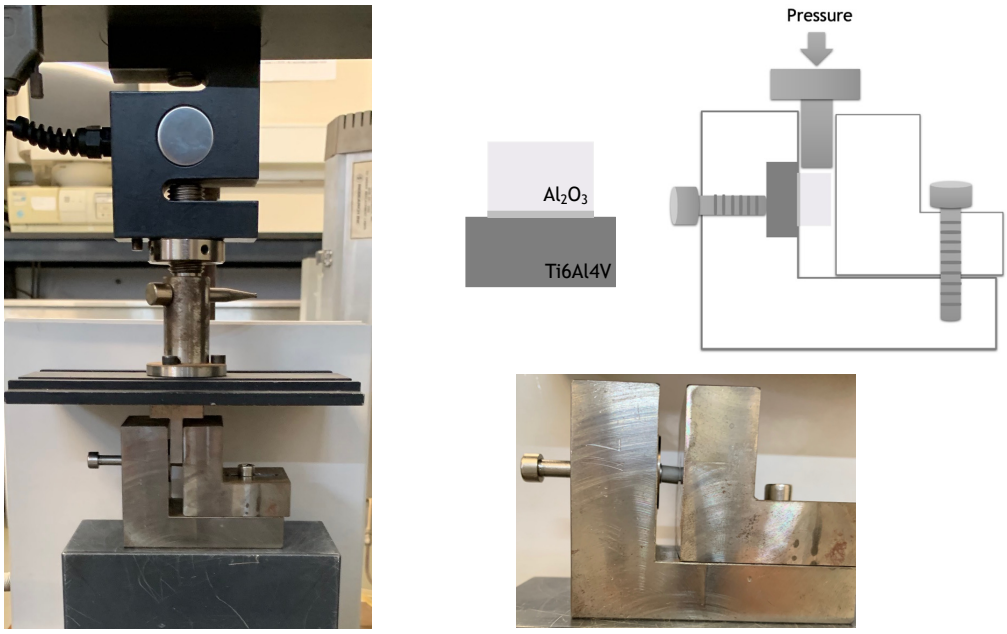

Figure 2. Shear strength test device and respective schematic illustration.

3. Results and Discussion

3.1. Ti Thin Films Deposited onto Al_2O_3

The adhesion of the Ti films to Al_2O_3 plays a vital role in the joints processed by diffusion bonding, and is affected by the surface topography of the Al_2O_3 substrate. Profilometry measured the substrate's surface roughness, and the results showed Ra values of 0.10 µm. Figure 3 shows the cross-section of the titanium thin film as deposited onto the surface of Al_2O_3. The Ti thin film is highlighted in light grey, and its total thickness is close to 1 µm, as desired. The adhesion pull-off test shows an average adhesion strength of 8 MPa, slightly below the 10 MPa referred to in the literature [48]. However, the thin films were not detached from the alumina substrate at the end of the experiments; only the interface glue/film was broken, which suggests that the adhesion strength is sufficient. Therefore, this value seems enough for the envisaged application.

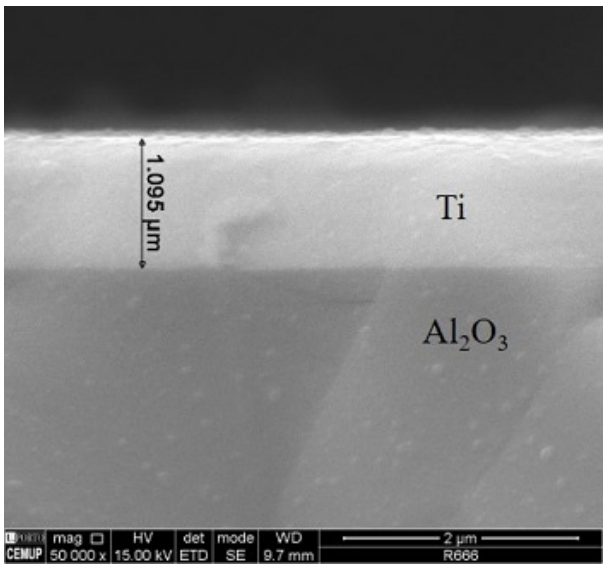

Figure 3. SEM image of the cross-section of as-deposited Ti thin film with total thickness close to 1 µm.

3.2. Diffusion Bonding without Interlayer

The joining between Ti6Al4V and Al_2O_3 without interlayer was only successful by diffusion bonding at 1000 °C with dwell times of 10 and 60 min with contact pressure. Figure 4 shows the cross-section of the joints interface. Some defects are observed in zones adjacent to alumina. This can be explained by the following factors: the lack of base materials surfaces' contact, the formation of brittle phases, or the development of residual stress, which promotes cracks during the cooling of the joints. The same defects were observed in joints obtained for both dwell times, 10 and 60 min. Figure 4b shows the interface in high magnification, and EDS analyzed zones highlighted in red. Figure 5 shows the SEM image of the interface produced for 10 min and the Ti, Al, and O EDS elemental distribution mapping. Despite the short bonding time, the EDS results show the occurrence diffusion of Al from Al_2O_3 and Ti and Al from Ti6Al4V to the interface. Zone Z1 in the vicinity of Ti6Al4V has contents of 78.9% Ti, 19.6% Al, and 1.5% V (at. %), combining the EDS results with ternary phase diagram [49], suggests the α-Ti phase is predominant. Zone Z2 comprises 73.3% Ti, 25.3% Al, and 1.4% V (at. %), and besides the α-Ti phase, the α_2-Ti_3Al phase may have also been formed. Some round and elongated particles near Al_2O_3 (Z3) have a chemical composition of 61.9% Ti, 36.6% Al, and 1.5% V and can be identified as γ-TiAl and α_2-Ti_3Al phases.

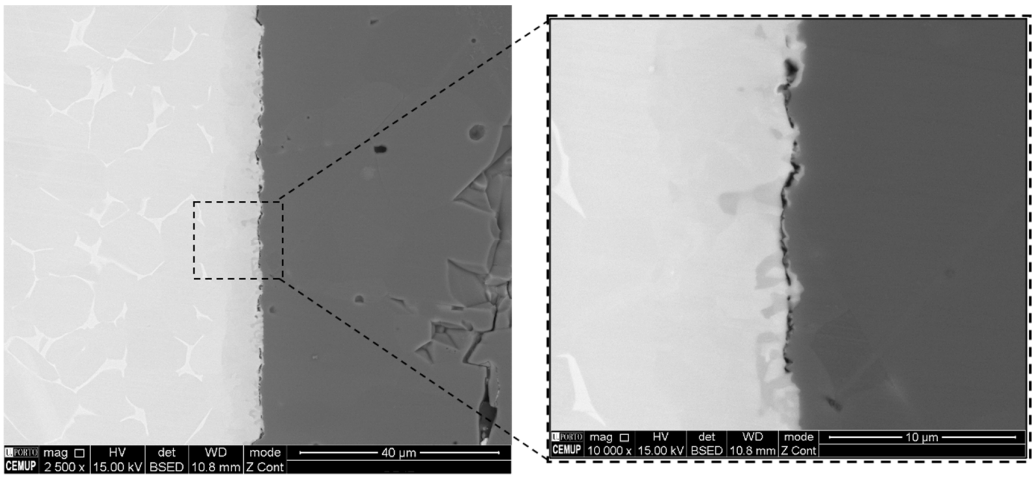

(**a**)

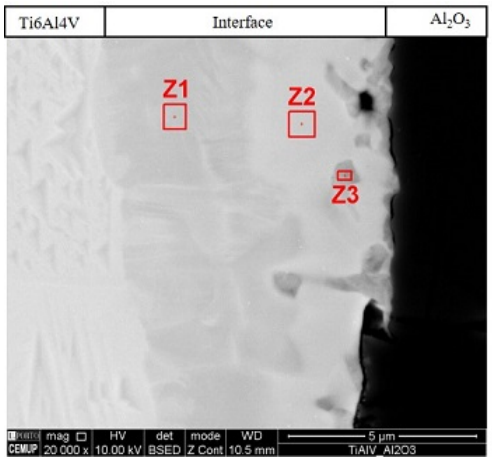

(**b**)

Figure 4. SEM images of the joints without interlayer processed at (**a**) 1000 °C for 60 min and (**b**) 1000 °C for 10 min.

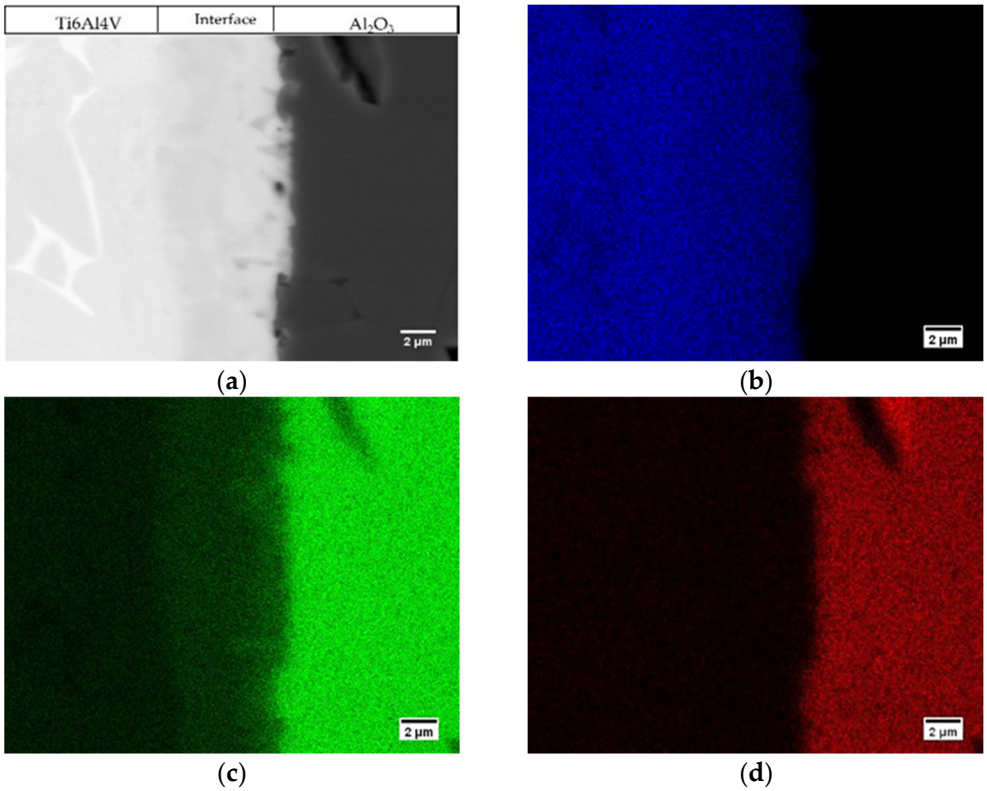

Figure 5. (**a**) SEM image and EDS elemental maps of (**b**) Ti, (**c**) Al, and (**d**) O of the interface obtained without interlayer at 1000 °C and dwell time of 10 min.

3.3. Diffusion Bonding Using Ti Thin Films Deposited onto Al_2O_3

The joining of dissimilar materials using interlayers on faying surfaces of the base materials is an approach to reduce the residual stresses in the diffusion bonding process and improve the contact between the faying surfaces [8,29,50–54]. Joining between Ti6Al4V and Al_2O_3 using Ti thin films deposited onto Al_2O_3 was performed at temperatures of 900, 950, and 1000 °C and dwell times of 10 and 60 min. Unsuccessful joints were obtained at 900 °C, for both bonding times, and joints processed at 950 °C for 10 min. The base materials were separated after cooling, proving that the diffusion bonding conditions were insufficient to promote the bonding of the dissimilar materials. Successful joints were obtained at 950 °C for 60 min and 1000 °C for 10 and 60 min with Ti thin film interlayer. Figure 6 shows SEM images of the interfaces of the joints processed under these conditions. Table 1 shows the EDS results of the zones marked on the SEM images of Figure 6. The identification of the possible phase(s) was performed by combining the EDS results with the Ti-Al-V phase diagram [49].

Figure 6a shows the joint processed at 950 °C and 60 min that exhibits an interface with a total thickness of ~15 µm, and the bond line is not visible. The interface can be divided into two distinct layers. The layer close to the Ti6Al4V (Z2) exhibits a chemical composition similar to the Ti base material (Z1), although slightly higher V content. Ti6Al4V is constituted by α-Ti phase (Z1) matrix with a β-Ti phase (Z4) rich in V at the grain boundaries. Combining the EDS results with the Ti-Al-V phase diagram, a layer of α-Ti phase can be identified. The layer adjacent to Al_2O_3 (Z3) has twice the Al content (22.5 at%) than that found in the layer adjacent to Ti6Al4V (10.2 at.% Al). The EDS results combined with the phase diagram suggest that this layer is mainly composed of the α_2-Ti_3Al phase. Close to Al_2O_3, darker particles were observed that could be identified as γ-TiAl (Z5).

Figure 6b shows the joint interface obtained at 1000 °C using a bonding time of 10 min. The interface has a thickness of ~13 µm, and two different layers are also observed. Despite the short bonding time, the bonding temperature promoted the formation of a sound

interface because the diffusion coefficient exponentially increases with temperature [55]. Identical to the interface produced at 950 °C, the layer adjacent to Ti6Al4V (Z3) is composed of α-Ti with a thickness of ~5 µm. The layer adjacent to Al_2O_3 (Z4), with a thickness of ~8 µm, has contents of 75.0 at.% Ti and 25.0 at.% Al suggesting that the Ti_3Al phase was formed during the diffusion bonding process. In-between the Al_2O_3 and this interface layer, it is possible to observe a thin layer (~1 µm) composed of alternated different grey columnar small grains. However, it was not possible to perform EDS analyses owing to its reduced thickness.

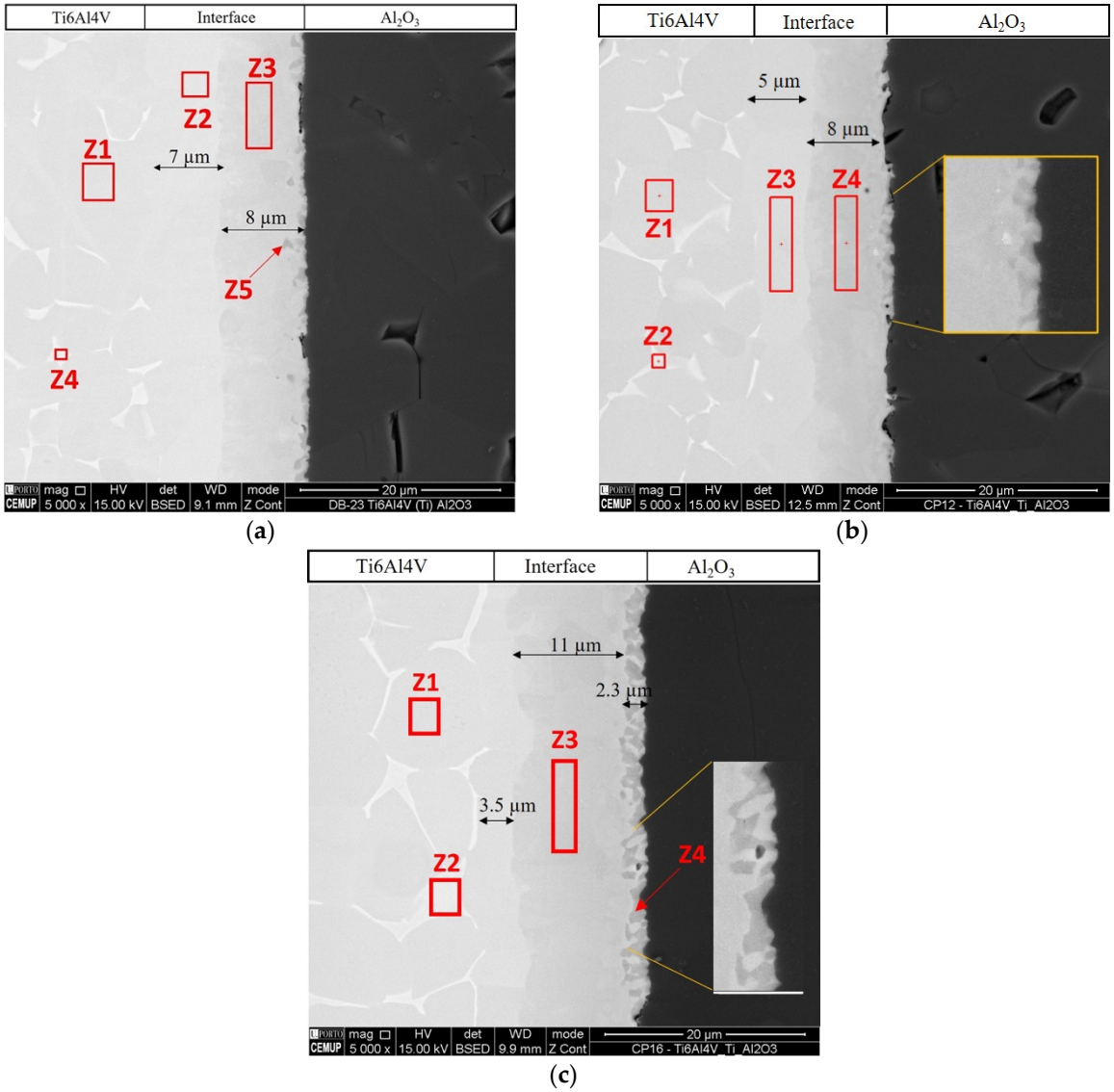

Figure 6. SEM images of the joints with Ti thin film interlayer processed at (**a**) 950 °C for 60 min, (**b**) 1000 °C for 10 min, and (**c**) 1000 °C for 60 min.

Increasing the bonding time at 1000 °C to 60 min promotes the change in the thickness of the layers that compose the interface. This interface can be observed in Figure 6c. The increase in the bonding time results in the decrease in the α-Ti phase and the growth of the Ti_3Al layer with TiAl particles close to Al_2O_3 (Z4 in Figure 6c).

The confirmation of the phases at the interfaces was conducted by EBSD, which allows Kikuchi patterns of tiny zones to be obtained due to the reduced interaction volume. Figure 7 shows EBSD Kikuchi patterns of the joint processed at 1000 °C for 60 min. This technique was of paramount importance to confirm the presence of the γ-TiAl intermetallic phase close to the Al_2O_3 base material.

Table 1. Chemical composition obtained by EDS of the zones in Figure 6.

Conditions	Zone	Element (at.%)			Possible Phases
		Ti	Al	V	
950 °C/60 min	1	88.5	10.3	1.2	α-Ti
	2	88.3	10.3	1.5	α-Ti
	3	76.5	22.5	1.0	α_2-Ti_3Al
	4	80.3	6.7	13.0	β-Ti
	5	65.1	33.7	1.2	α_2-Ti_3Al + γ-TiAl
1000 °C/10 min	1	86.8	11.6	1.6	α-Ti
	2	73.3	19.7	7.0	β-Ti
	3	86.0	11.9	2.1	α-Ti
	4	75.0	25.0	*	α_2-Ti_3Al
1000 °C/60 min	1	88.3	11.7	*	α-Ti
	2	77.1	6.9	16.0	β-Ti
	3	74.5	25.5	*	α_2-Ti_3Al
	4	57.6	42.4	*	α_2-Ti_3Al + γ-TiAl

*—not detected.

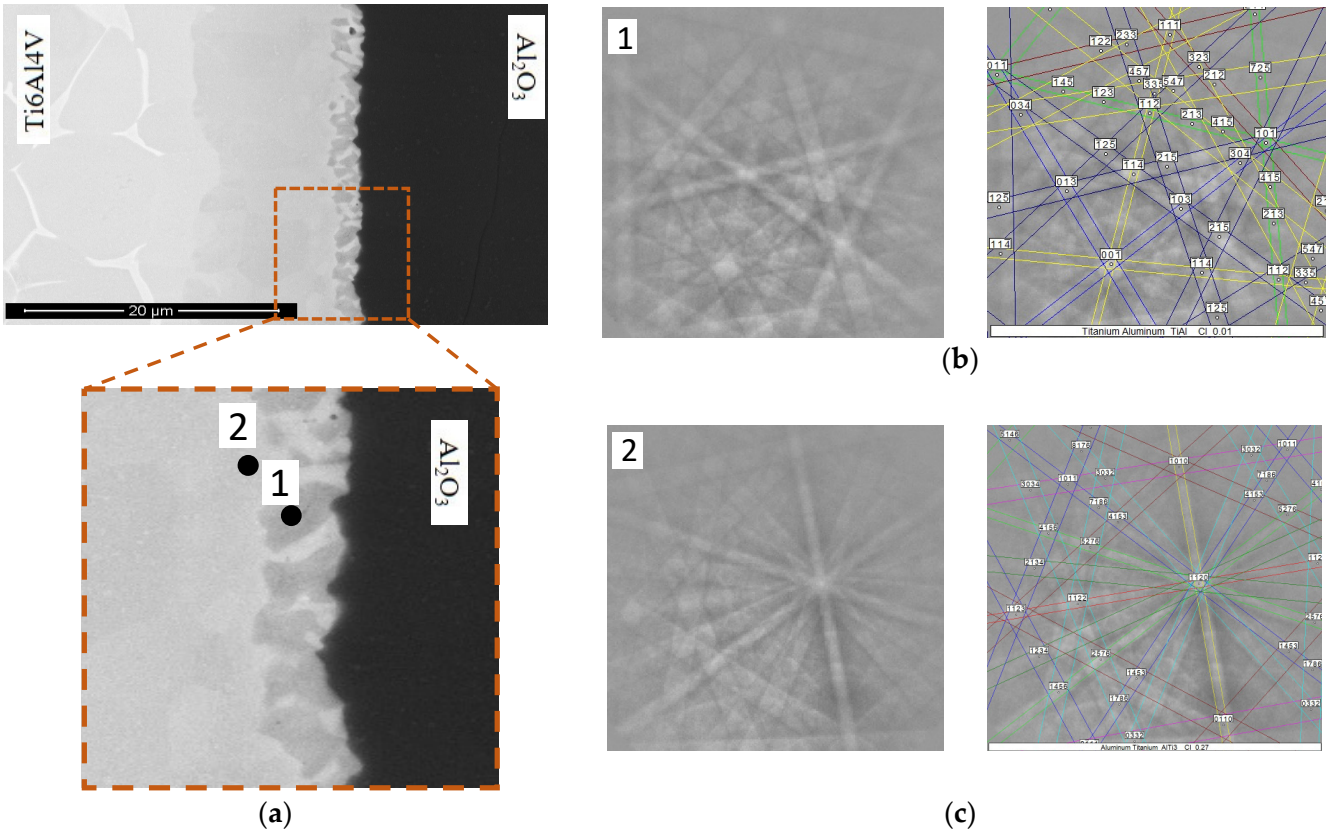

Figure 7. (**a**) SEM images of the interface produced with Ti thin film processed at 1000 °C for 60 min, (**b**) EBSD Kikuchi patterns of the grain marked as 1 in (**a**) indexed as γ-TiAl, and (**c**) EBSD Kikuchi patterns of the grain marked as 2 in (**a**) indexed as α_2-Ti_3Al.

The nanoindentation experiments were performed across the joints interface and adjacent base materials. Hardness and reduced Young's modulus (E_r) maps were obtained to understand their distribution across the joints interface (Figure 8). The reduced Young's modulus map is only shown for the joint interface processed at 1000 °C for 60 min. The different hardness values allow the base materials to be identified, as well as the interface. As expected, the Al_2O_3 displays the highest hardness value, around 30–50 GPa. The interface hardness is similar to that of titanium alloy but increases slightly near the Al_2O_3

base material. The increase in temperature and time of diffusion bonding promotes an increase in the hardness of the interface that is in accordance with the microstructural characterization. The increase in the diffusion bonding temperature or time induces the increase in the thickness of the α_2-Ti_3Al and α_2-Ti_3Al + γ-TiAl layers, which can be associated with the increase in the hardness.

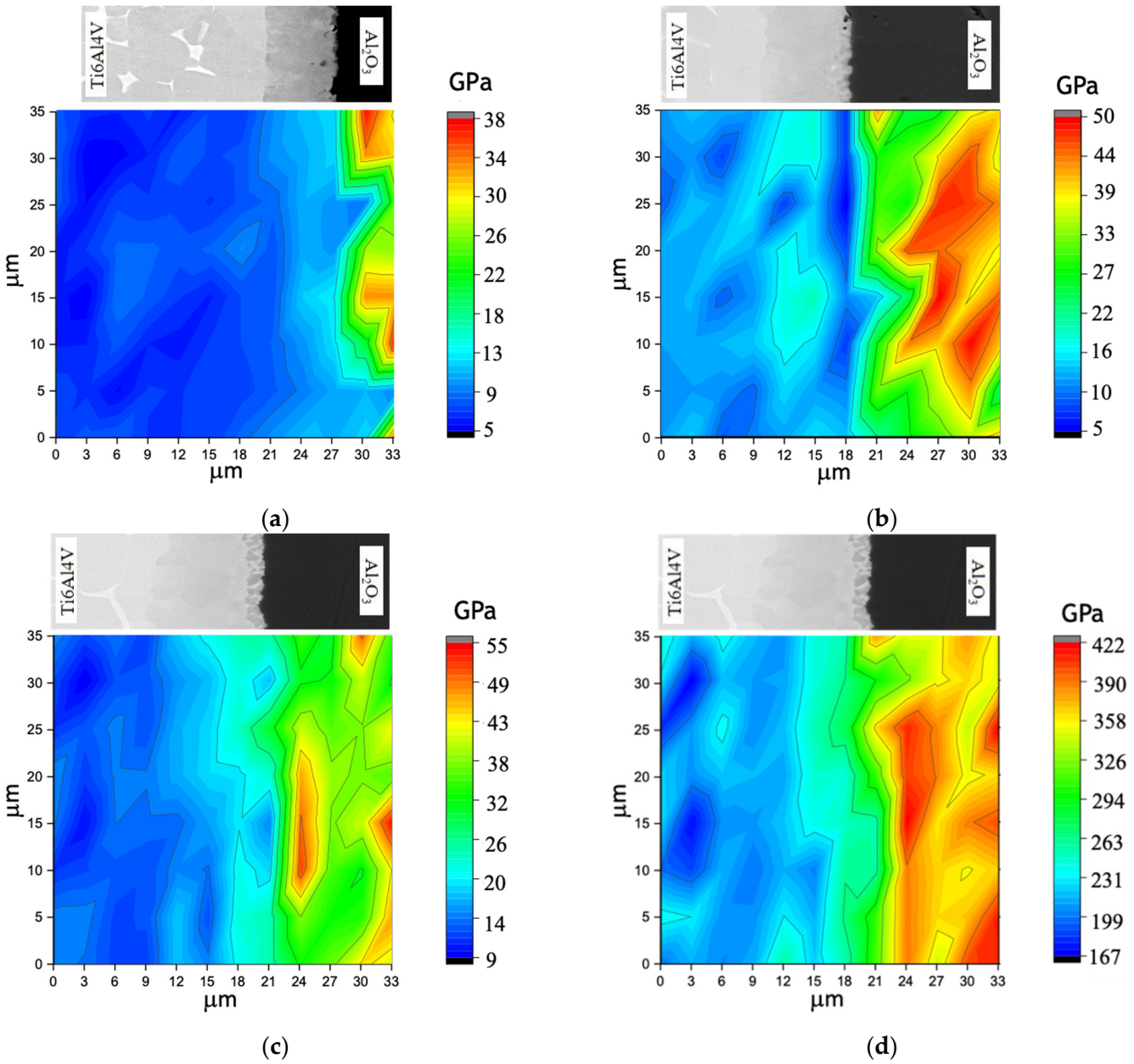

Figure 8. (**a**–**c**) Hardness maps of the joints processed at 950 °C for 60 min, 1000 °C for 10 min, and 1000 °C for 60 min, respectively, and (**d**) reduced Young's modulus map across the joint processed at 1000 °C for 60 min.

Regarding the reduced Young's modulus, the map (Figure 8d) allows the different regions to be distinguished from the lower values (Ti6Al4V) towards, the higher values (Al_2O_3), passing by the two interface layers. The thicker layer corresponding to α_2-Ti_3Al has a slightly higher modulus than the Ti alloy base material, while the thinner layer (α_2-Ti_3Al + γ-TiAl) has an even higher modulus (Figure 8d). The Al_2O_3 base material has the highest reduced Young's modulus.

The shear strength of the joints was evaluated by shear tests. Table 2 displays the values of the shear strength of the joints processed at 1000 °C for 60 min, with and without

interlayers, and at 950 °C for 60 min with an interlayer (Ti thin film). At 950 °C, only two values are presented because, for the third sample, during the test, the sample was fractured but fitted in the support, and the computer continued to record the force—this test being considered invalid. The average shear strength values are very similar for the samples processed at 1000 °C for 60 min (52 ± 14 MPa for the joint processed without interlayer and 49 ± 25 MPa for the joint processed with interlayer). In fact, the use of the Ti interlayer allows the decrease in the bonding conditions without impairing the mechanical properties. This can be explained since the microstructure of the interface is very similar, and the interface is composed of the same phases. The Ti thin films improve the adhesion to the ceramic base material and, due to the fine microstructure, enhance the diffusion across the interface during the joining process. These results confirm that these interlayers improve the bonding process of these dissimilar materials.

Figure 9 presents the fracture surface of the samples with higher and lower shear strength values. It can be observed that when the fracture occurs at the ceramic base material, the shear strength is higher. The fracture occurs at the Al_2O_3 and then propagates to the interface (Figure 9a). On the contrary, when the fracture occurs at the interface and propagates through the interface, the shear strength value is lower, (Figure 9b). This happen when the joint presents some defects at the interface, such as pores in the layer close to the Al_2O_3, that promote the nucleation of the fissure at the interface.

Table 2. Shear strength values of the joints produced without interlayer at 1000 °C for 60 min and with Ti thin film at 1000 and 950 °C for 60 min.

Joint Processing Conditions	Interlayers	Shear Strength (MPa)
1000 °C for 60 min	without	66 54 38
1000 °C for 60 min	Ti thin film	77 41 27
950 °C for 60 min	Ti thin film	43 [1] 30

[1]—only two values are present since one test was considered invalid.

Based on the reaction between the Ti thin film and the base materials observed at different diffusion bonding temperatures and times, a common mechanism can be pointed out to explain the formation of the interface microstructure during the joining of Al_2O_3 to Ti6Al4V alloy. Figure 10 shows a schematic illustration of a possible mechanism for the formation of the interfaces, as well as the microstructure of the interface obtained at different temperatures and times. During the bonding process, due to the temperature increase, the Ti of the film starts to diffuse from the film towards the base materials, while the Ti and Al of the Ti alloy and the Al of the ceramic diffuse towards the interface. The Ti film at the interface starts to grow significantly, and this is also due to the fine grain microstructure of the film because it is produced by magnetron sputtering, which enhances diffusion. The Al diffusing from the Al_2O_3 will combine with the Ti at the interface and form a layer of α_2-Ti_3Al. With increasing diffusion due to higher temperature and time, the α_2-Ti_3Al layer thickness will increase. At high temperatures and long times, diffusion will result in a thicker α_2-Ti_3Al layer and the formation of alternating α_2-Ti_3Al and γ-TiAl grains along the Al_2O_3 base material. During cooling, different microstructures will form, which are represented in Figure 10d–f. The thickness of the layers that compose the interfaces depend on the temperature and time of diffusion bonding, since this process is ensured by the diffusion of the elements that react and form the different reaction layers.

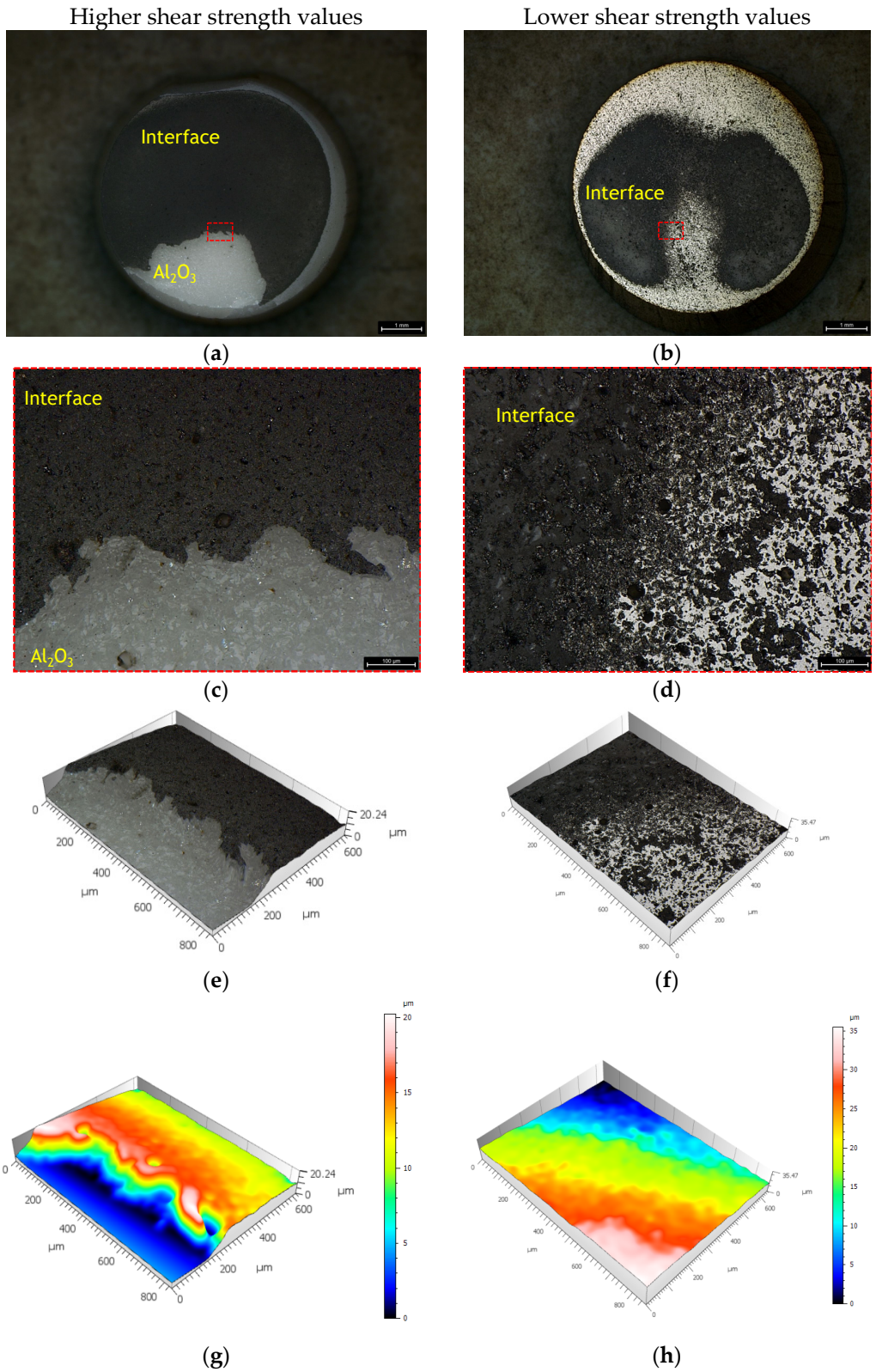

Figure 9. Fracture surface of the joints with (**a**,**c**,**e**,**g**) higher and (**b**,**d**,**f**,**h**) lower shear strength values: (**a**,**b**) low magnification of the Al_2O_3 samples, (**c**,**d**) high magnification of the regions marked in (**a**,**b**), respectively, (**e**–**h**) 3D representation of regions (**c**,**d**).

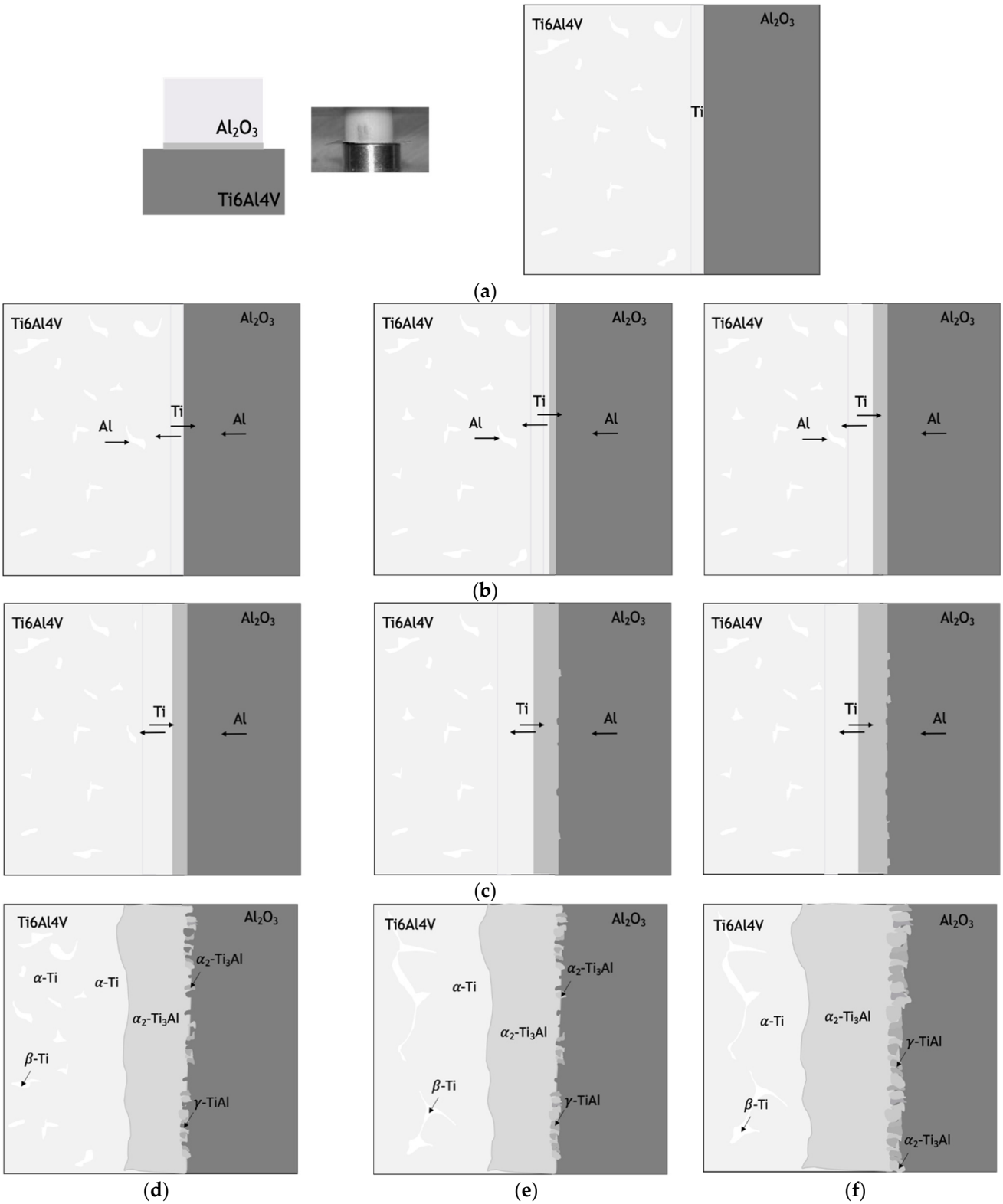

Figure 10. Microstructure evolution during the diffusion bonding of Ti6Al4V to Al_2O_3 using Ti thin films: (**a**) initial microstructure, (**b**) sequence of the formation and growth of the α_2-Ti_3Al layer due to Ti and Al diffusion, (**c**) growth of α-Ti, formation of α_2-Ti_3Al layer and formation of α_2-Ti_3Al and γ-TiAl grains close to Al_2O_3 base material, (**d**) microstructure of the interface formed at 950 °C for 60 min, (**e**) microstructure of the interface formed at 1000 °C for 10 min and (**f**) microstructure of the interface formed at 1000 °C for 60 min.

3.4. Diffusion Bonding with Freestanding Ti Thin Foils

Diffusion bonding experiments of Ti6Al4V to Al_2O_3 using 5 µm freestanding Ti foils were performed at 950 °C for 10 and 60 min. The joining was unsucessful under these bonding conditions. Figure 11 shows OM images of the interface produced at 950 °C for 60 min. Based on these images, the lack of joint between the Ti foil and the Al_2O_3 base material is clear. In addition, between the Ti foil and the Ti6Al4V alloy, there are also unbounded areas that can be observed. These results suggest that the bonding conditions are not sufficient to promote the joining between dissimilar materials, revealing that having the Al_2O_3 base material coated with Ti thin films is a more promising approach. The films deposited on Al_2O_3 are crucial to guarantee the adhesion between the Ti interlayer and the ceramic material. This adhesion is essential for the success of the ceramic/metal solid state diffusion bonding process. Furthermore, the fine microstructure of the thin film deposited by sputtering seems to be a parameter to take into account. The bond between the Ti foil and the Ti6Al4V alloy also fails, showing that this interlayer does not present the requisites to be applied in the diffusion bonding process under study.

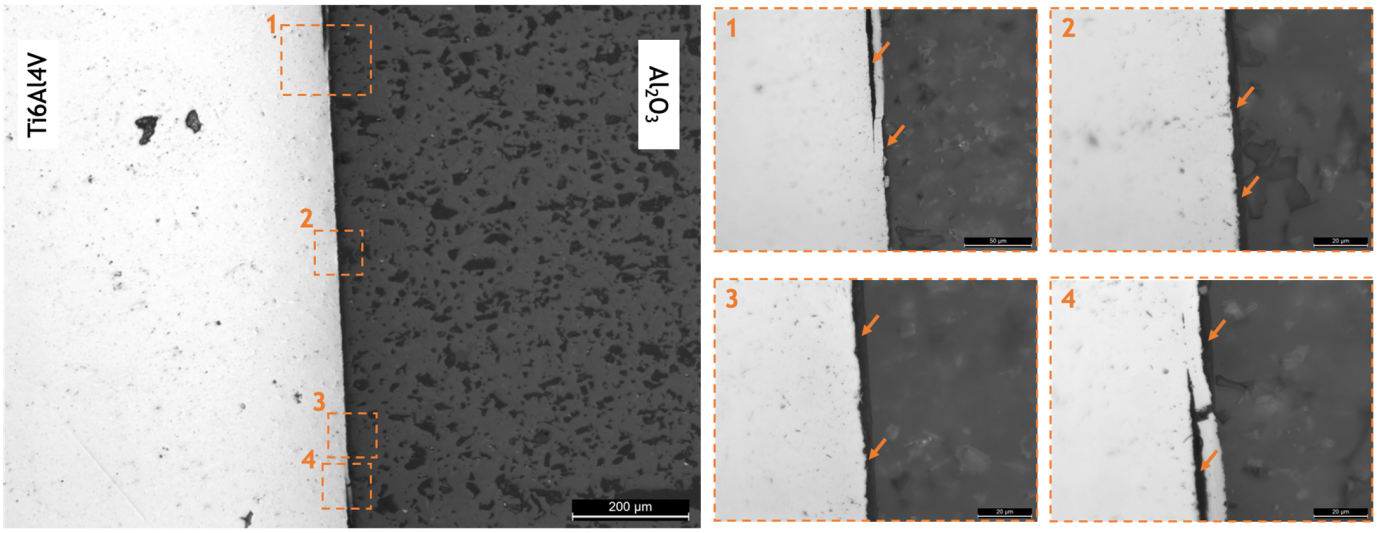

Figure 11. OM images of the joint processed at 950 °C for 60 min using a Ti freestanding thin foil as interlayer.

4. Conclusions

Diffusion bonding of Ti6Al4V to Al_2O_3 using titanium as interlayer was investigated in this work. Two different interlayers were considered to evaluate the effect of the adhesion during the diffusion bonding process. Sputtered Ti thin films (1 µm) deposited onto Al_2O_3 base material and commercial freestanding titanium foils (5 µm) were used for this purpose. Without interlayers, the diffusion bonding experiments were only achieved at 1000 °C for 10 and 60 min. However, some defects are observed close to the ceramic base material. Using Ti films with ~1 µm thickness, the contact between the base materials was improved, allowing sound joints to be obtained at 950 °C for 60 min. The joining interface was characterized by α-Ti, α_2-Ti_3Al and γ-TiAl phases. The increase in the joining temperature and time promote the increase in the thickness of the layers at the interface. An intense diffusion is observed, and the fine microstructure of the thin film seems to improve the diffusion bonding process. The use of Ti freestanding films was unsuccessful, proving that the adhesion to the ceramic material is a crucial aspect for this approach. The hardness maps confirm the microstructural results, revealing that the interface exhibited a hardness similar to the Ti6Al4V, but it increases with the increase in temperature and time of the diffusion bonding process. The average shear strength values are similar for all joints tested, confirming that the use of the Ti thin film improves the diffusion bonding of the

Ti6Al4V alloy to alumina, promoting a decrease in the temperature and time required to achieve sound ceramic/metal joining.

Author Contributions: Conceptualization, M.S.J.; methodology, S.S. and A.S.R.; validation, S.S. and A.S.R.; investigation, M.S.J., S.S. and A.S.R.; writing—original draft preparation M.S.J.; writing—review and editing, S.S. and A.S.R.; Supervision, S.S. and A.S.R.; funding acquisition, S.S. All authors have read and agreed to the published version of the manuscript.

Funding: This work was financially supported by: Project PTDC/CTM-CTM/31579/2017—POCI-01-0145-FEDER-031579—funded by FEDER funds through COMPETE2020—Programa Operacional Competitividade e Internacionalização (POCI) and by national funds (PIDDAC) through FCT/MCTES. This research was also supported by FEDER funds through the program COMPETE—Programa Operacional Factores de Competitividade, and by national funds through FCT—Fundação para a Ciência e a Tecnologia, under the project UIDB/EMS/00285/2020.

Data Availability Statement: Data can be available upon request from the authors.

Acknowledgments: The authors are grateful to CEMUP-Centre of Materials of the University of Porto for expert assistance with SEM.

Conflicts of Interest: The authors declare no conflict of interest.

References

1. *Titanium and Titanium Alloys*; Leyens, C.; Peters, M. (Eds.) Wiley: Hoboken, NJ, USA, 2003; ISBN 9783527305346.
2. Carter, C.B.; Norton, M.G. *Ceramic Materials*; Springer: New York, NY, USA, 2007; ISBN 978-0-387-46270-7.
3. Simões, S. Recent Progress in the Joining of Titanium Alloys to Ceramics. *Metals* **2018**, *8*, 876. [CrossRef]
4. Li, H.; Ma, Y.; Xu, B.; Bridges, D.; Zhang, L.; Feng, Z.; Hu, A. Laser welding of Ti6Al4V assisted with nanostructured Ni/Al reactive multilayer films. *Mater. Des.* **2019**, *181*, 108097. [CrossRef]
5. Kaneko, A.; Katayama, T.; Morishita, S. Micro Fabrication of Au Thin-Film by Transfer-Printing Using Atomic Diffusion Bonding. *Int. J. Autom. Technol.* **2019**, *13*, 810–816. [CrossRef]
6. Cazajus, V.; Seguy, S.; Welemane, H.; Karama, M. Residual Stresses in a Ceramic-Metal Composite. *Appl. Mech. Mater.* **2012**, *146*, 185–196. [CrossRef]
7. Shi, G.; Zhang, L.; Wang, Z. Modelling the Elements Reaction–Diffusion Behavior on Interface of Ti/Al_2O_3 Composite Prepared by Hot Pressing Sintering. *Metals* **2020**, *10*, 259. [CrossRef]
8. Misra, A.K. Reaction of Ti and Ti-Al alloys with alumina. *Met. Mater. Trans. A* **1991**, *22*, 715–721. [CrossRef]
9. Lu, Y.-C.; Sass, S.; Bai, Q.; Kohlstedt, D.; Gerberich, W. The influence of interfacial reactions on the fracture toughness of Ti-Al_2O_3 interfaces. *Acta Met. Mater.* **1995**, *43*, 31–41. [CrossRef]
10. Yu, W.; Zhao, H.; Huang, Z.; Chen, X.; Aman, Y.; Li, S.; Zhai, H.; Guo, Z.; Xiong, S. Microstructure evolution and bonding mechanism of Ti_2SnC-Ti6Al4V joint by using Cu pure foil interlayer. *Mater. Charact.* **2017**, *127*, 53–59. [CrossRef]
11. Loh, N.L.; Wu, Y.L. Diffusion bonding of ceramic to metals. *Mater. Manuf. Proc.* **1993**, *8*, 159–181. [CrossRef]
12. Nicholas, M.G.; Crispin, R.M. Diffusion bonding stainless steel to alumina using aluminium interlayers. *J. Mater. Sci.* **1982**, *17*, 3347–3360. [CrossRef]
13. Yin, X.; Li, M.; Zhou, Y. Microstructure and mechanical strength of diffusion-bonded Ti_3SiC_2/Ni joints. *J. Mater. Res.* **2006**, *21*, 2415–2421. [CrossRef]
14. Hattali, M.; Valette, S.; Ropital, F.; Mesrati, N.; Tréheux, D. Interfacial behavior on Al_2O_3/HAYNES® 214™ joints fabricated by solid state bonding technique with Ni or Cu–Ni–Cu interlayers. *J. Eur. Ceram. Soc.* **2012**, *32*, 2253–2265. [CrossRef]
15. Uday, M.B.; Ahmad-Fauzi, M.N.; Noor, A.M.; Rajoo, S. Current Issues and Problems in the Joining of Ceramic to Metal. In *Joining Technologies*; Ishak, M., Ed.; InTech: Rijeka, Croatia, 2016; Chapter 8.
16. Elssner, G.; Petzow, G. Metal/ceramic joining. *ISIJ Int.* **1990**, *30*, 1011–1032. [CrossRef]
17. Zhang, Y.; Feng, D.; He, Z.-Y.; Chen, X.-C. Progress in Joining Ceramics to Metals. *J. Iron Steel Res. Int.* **2006**, *13*, 1–5. [CrossRef]
18. Yang, Z.; Lin, J.; Wang, Y.; Wang, D. Characterization of microstructure and mechanical properties of Al_2O_3/TiAl joints vacuum-brazed with Ag-Cu-Ti + W composite filler. *Vacuum* **2017**, *143*, 294–302. [CrossRef]
19. Cao, J.; Zheng, Z.; Wu, L.; Qi, J.; Wang, Z.; Feng, J. Processing, microstructure and mechanical properties of vacuum-brazed Al_2O_3/Ti6Al4V joints. *Mater. Sci. Eng. A* **2012**, *535*, 62–67. [CrossRef]
20. Niu, G.; Wang, D.; Yang, Z.; Wang, Y. Microstructure and mechanical properties of Al_2O_3/TiAl joints brazed with B powders reinforced Ag-Cu-Ti based composite fillers. *Ceram. Int.* **2017**, *43*, 439–450. [CrossRef]
21. Xue, H.; Wei, X.; Guo, W.; Zhang, X. Bonding mechanism study of active Ti element and α-Al_2O_3 by using first-principle calculation. *J. Alloys Compd.* **2020**, *820*, 153070. [CrossRef]
22. Qiu, Q.; Wang, Y.; Yang, Z.; Wang, D. Microstructure and mechanical properties of Al_2O_3 ceramic and Ti6Al4V alloy joint brazed with inactive Ag–Cu and Ag–Cu + B. *J. Eur. Ceram. Soc.* **2016**, *36*, 2067–2074. [CrossRef]

23. Wang, Z.M.; Yang, J.H.; Qi, F.Q.; Hou, A.L.; Yang, Z.W.; Wang, Y.; Wang, D.P. Interfacial characterization and mechanical properties of reactive air brazed ZrO_2 ceramic joints with Ag-CuO-Al_2TiO_5 composite filler metal. *Ceram. Int.* **2021**, *47*, 29128–29138. [CrossRef]
24. Xin, C.; Yan, J.; Li, N.; Liu, W.; Du, J.; Cao, Y.; Shi, H. Microstructural evolution during the brazing of Al_2O_3 ceramic to kovar alloy by sputtering Ti/Mo films on the ceramic surface. *Ceram. Int.* **2016**, *42*, 12586–12593. [CrossRef]
25. Dai, X.; Cao, J.; Liu, J.; Wang, D.; Feng, J. Interfacial reaction behavior and mechanical characterization of ZrO_2/TC4 joint brazed by Ag–Cu filler metal. *Mater. Sci. Eng. A* **2015**, *646*, 182–189. [CrossRef]
26. Barbier, F.; Peytour, C.; Revcolevschi, A. Microstructural Study of the Brazed Joint between Alumina and Ti-6AI-4V Alloy. *J. Am. Ceram. Soc.* **1990**, *73*, 1582–1586. [CrossRef]
27. Emadinia, O.; Guedes, A.; Tavares, C.; Simões, S. Joining Alumina to Titanium Alloys Using Ag-Cu Sputter-Coated Ti Brazing Filler. *Materials* **2020**, *13*, 4802. [CrossRef]
28. Peytour, C.; Barbier, F.; Revcolevschi, A. Characterization of ceramic/TA6V titanium alloy brazed joints. *J. Mater. Res.* **1990**, *5*, 127–135. [CrossRef]
29. Mishra, S.; Sharma, A.; Jung, D.H.; Jung, J.P. Recent Advances in Active Metal Brazing of Ceramics and Process. *Met. Mater. Int.* **2019**, *26*, 1087–1098. [CrossRef]
30. Akselsen, O.M. Diffusion bonding of ceramics. *J. Mater. Sci.* **1992**, *27*, 569–579. [CrossRef]
31. Simões, S.; Viana, F.; Ramos, A.S.; Vieira, M.T. Microstructural Characterization of Dissimilar Titanium Alloys Joints Using Ni/Al Nanolayers. *Metals* **2018**, *8*, 715. [CrossRef]
32. Simões, S.; Viana, F.; Ramos, A.S.; Vieira, M. Diffusion Bonding of TiAl to Ti6Al4V Using Nanolayers. *J. Mater. Eng. Perform.* **2018**, *27*, 5064–5068. [CrossRef]
33. Simões, S.; Viana, F.; Koçak, M.; Ramos, A.S.; Vieira, M. Diffusion bonding of TiAl using reactive Ni/Al nanolayers and Ti and Ni foils. *Mater. Chem. Phys.* **2011**, *128*, 202–207. [CrossRef]
34. Aucott, L.; Bamber, R.; Lunev, A.; Darby, T.; Maquet, P.; Gimbert, N.; Pak, S.; Walsh, M.; Udintsev, V.; Eaton, G.; et al. Solid-State Diffusion Bonding of Glass-Metal for the International Thermonuclear Experimental Reactor (ITER) Diagnostic Windows. In *TMS 2020 149th Annual Meeting & Exhibition Supplemental Proceedings*; Springer International Publishing: Cham, Switzerland, 2020; pp. 2085–2094.
35. Cavaleiro, A.; Ramos, A.; Fernandes, F.B.; Schell, N.; Vieira, M. Follow-up structural evolution of Ni/Ti reactive nano and microlayers during diffusion bonding of NiTi to Ti6Al4V in a synchrotron beamline. *J. Mater. Process. Technol.* **2020**, *275*, 116354. [CrossRef]
36. Weiqi, Y.; Jincheng, L.; Run, A.; Lili, X. High shear strength and ductile ZrC–SiC/austenitic stainless steel joints bonded with Ti/Ni foam interlayer. *Ceram. Int.* **2020**, *46*, 3036–3042. [CrossRef]
37. Niu, J.B.; Wang, Y.; Yang, Z.W.; Wang, D.P. Microstructure and Mechanical Properties of Titanium–Zirconium–Molybdenum and Ti_2AlNb Joint Diffusion Bonded with and without a Ni Interlayer. *Adv. Eng. Mater.* **2019**, *21*, 1900713. [CrossRef]
38. Wang, Q.; Chen, G.-Q.; Wang, K.; Fu, X.-S.; Zhou, W.-L. Microstructural evolution and growth kinetics of interfacial compounds in TiAl/Ti_3SiC_2 diffusion bonding joints. *Mater. Sci. Eng. A* **2019**, *756*, 149–155. [CrossRef]
39. Zhang, Y.; Chen, Y.; Yu, D.; Sun, D.; Li, H. A review paper on effect of the welding process of ceramics and metals. *J. Mater. Res. Technol.* **2020**, *9*, 16214–16236. [CrossRef]
40. Barrena, M.; Matesanz, L.; de Salazar, J.G. Al_2O_3/Ti6Al4V diffusion bonding joints using Ag–Cu interlayer. *Mater. Charact.* **2009**, *60*, 1263–1267. [CrossRef]
41. Kliauga, A.; Ferrante, M. Interface compounds formed during the diffusion bonding of Al_2O_3 to Ti. *J. Mater. Sci.* **2000**, *35*, 4243–4249. [CrossRef]
42. Travessa, D.; Ferrante, M. The Al_2O_3-t itanium adhesion in the view of the diffusion bonding process. *J. Mater. Sci.* **2002**, *37*, 4385–4390. [CrossRef]
43. Rocha, L.; Ariza, E.; Costa, A.M.; Oliveira, F.J.; Silva, R.F. Electrochemical behavior of Ti/Al_2O_3 interfaces produced by diffusion bonding. *Mater. Res.* **2003**, *6*, 439–444. [CrossRef]
44. Heikinheimo, L.S.K.; De With, G. *Interface Structure and Fracture Energy of Al_2O_3-Ti Joints: Dissertation*; VTT Technical Research Centre of Finland: Espoo, Finland, 1995.
45. Lim, J.D.; Lee, P.M.; Chen, Z. Understanding the bonding mechanisms of directly sputtered copper thin film on an alumina substrate. *Thin Solid Film.* **2017**, *634*, 6–14. [CrossRef]
46. Silva, M.; Ramos, A.; Vieira, M.; Simões, S. Diffusion Bonding of Ti6Al4V to Al_2O_3 Using Ni/Ti Reactive Multilayers. *Metals* **2021**, *11*, 655. [CrossRef]
47. Oliver, W.; Pharr, G. An improved technique for determining hardness and elastic modulus using load and displacement sensing indentation experiments. *J. Mater. Res.* **1992**, *7*, 1564–1583. [CrossRef]
48. Lim, J.D.; Lee, P.M.; Rhee, D.M.W.; Leong, K.C.; Chen, Z. Effect of surface treatment on adhesion strength between magnetron sputtered copper thin films and alumina substrate. *Appl. Surf. Sci.* **2015**, *355*, 509–515. [CrossRef]
49. Hayes, F.H. The Al-Ti-V (aluminum-titanium-vanadium) system. *J. Phase Equilibria Diffus.* **1995**, *16*, 163–176. [CrossRef]
50. Zhu, S.; Włosiński, W. Joining of AlN ceramic to metals using sputtered Al or Ti film. *J. Mater. Process. Technol.* **2001**, *109*, 277–282. [CrossRef]

51. Valenza, F.; Artini, C.; Passerone, A.; Cirillo, P.; Muolo, M.L. Joining of ZrB_2 Ceramics to Ti6Al4V by Ni-Based Interlayers. *J. Mater. Eng. Perform.* **2014**, *23*, 1555–1560. [CrossRef]
52. Zhang, X.; Lu, G. Properties and Interface Structures of Ni and Ni-Ti Alloy Toughened $A1_2O_3$ Ceramic Composites. *J. Eur. Ceram. Soc.* **1994**, *15*, 225–232. [CrossRef]
53. Lu, Y.; Zhu, M.; Zhang, Q.; Hu, T.; Wang, J.; Zheng, K. Microstructure evolution and bonding strength of the Al_2O_3/Al_2O_3 interface brazed via Ni-Ti intermetallic phases. *J. Eur. Ceram. Soc.* **2020**, *40*, 1496–1504. [CrossRef]
54. Yi, J.; Zhang, Y.; Wang, X.; Dong, C.; Hu, H. Characterization of Al/Ti Nano Multilayer as a Jointing Material at the Interface between Cu and Al_2O_3. *Mater. Trans.* **2016**, *57*, 1494–1497. [CrossRef]
55. Gietzelt, T.; Toth, V.; Huell, A. Diffusion Bonding: Influence of Process Parameters and Material Microstructure. In *Joining Technologies*; Intech Open Publishers: London, UK, 2016; pp. 195–216. [CrossRef]